Hindawi
Mathematical Problems in Engineering
Volume 2022, Article ID 7829827, 7 pages
https://doi.org/10.1155/2022/7829827

Research Article

Fitting the Relaxation Modulus of Viscoelastic Materials Based on the IoT-Supported Mathematics Algorithm

Lunlun Wan and Fuyan Lin

China University of Mining & Technology (Beijing), School of Mechatronics and Information Engineering, Haidian, Beijing 100083, China

Correspondence should be addressed to Lunlun Wan; bqt2000401004@student.cumtb.edu.cn

Received 11 January 2022; Accepted 25 January 2022; Published 14 February 2022

Academic Editor: Gengxin Sun

In this paper, the theory of viscoelastic material relaxation modulus testing, testing method, and material relaxation modulus parameter solution method is studied. Based on the IoT sensor test devices and the Hertzian mathematics theory, the relationship between the compression amount, pressure, and relaxation modulus of a rigid spherical indenter pressed into a flat viscoelastic material is studied. In combination with the Boltzmann superposition principle, the relaxation modulus test method and theory for viscoelastic materials are proposed. A good fitting curve was obtained to solve the relaxation modulus parameters of various materials under the three-element Maxwell model. The experimental setup and the results of the parameter fitting were analyzed to verify the feasibility and accuracy of the results.

1. Introduction

Coal has always accounted for more than 70% of China's primary energy output and consumption, and is an important factor in ensuring national energy security [1]. In recent years, due to the domestic and international economic environment and the impact of the new epidemic, the coal economy has experienced a downward trend to vary degrees [2]. In December, the national coal output reached 340 million tons, a year-on-year decrease of 5.18%. In the first of July, the coal output totaled 2.066 billion tons, a year-on-year decrease of 7.18%. Nevertheless, coal industry is still one of the pillar industries of China's economy. China's development strategy has a reasonable plan for the medium and long-term goals of coal energy, and the structural share of coal in the energy mix will be controlled at 62% in 2020 and 55% in 2030 [3]. It can be seen that the position and role of coal in China's energy structure will not be changed for a long period of time in the future [4]. As an important economic pillar, the transformation and improvement of the coal industry are urgent [5]. The progress of science and technology is the key to the transformation and upgrading of the coal industry, among which the improvement and upgrading of coal machinery are particularly important [6]. Among the coal mining machinery, a belt conveyor is responsible for the transportation of coal from the surface to the underground and is an important transportation machine for coal production [7]. The technology level of the belt conveyor has a great influence on the operating cost of the enterprise and the efficiency of coal delivery. In recent years, although some coal mining machines such as coal miners and hydraulic supports have been greatly improved in China, the improvement and research of belt conveyors have been slow, especially in reducing energy consumption [8]. Nowadays, many belt conveyors have the characteristics of high speed, large capacity, and long-distance transportation, and they are bound to develop in the direction of higher speed, larger capacity, and longer distance in the future [9], so the issue of how to reduce energy consumption must be considered when manufacturing and developing belt conveyors [10]. The resistance to the operation of the belt conveyor largely influences the amount of energy consumed in its operation. Its resistance in a steady state of operation broadly includes additional resistance, main resistance,

special resistance, and angular inclination resistance [11]. Among them, the most influential operating resistance is the main resistance. The main resistance includes the rotational resistance of the rollers, the indentation resistance caused by the contact between the rollers and the conveyor belt, the resistance caused by the repeated bending and deformation of the conveyor belt, the friction resistance of the sweeper, and the redirection resistance of the conveyor belt.

Among the many operating resistances, the two resistances that have the greatest impact on the energy consumption of a belt conveyor are the rotational resistance of the rollers and the indentation resistance caused by the contact between the rollers and the conveyor belt [12]. According to the data [13], the rotational resistance of the rollers accounts for about 9% of the operating resistance, and the indentation resistance caused by the contact between the rollers and the conveyor belt accounts for about 61% of the operating resistance of a high-powered belt conveyor with a length of 1 km and high speed. According to this, the indentation resistance generated by the contact between the rollers and the conveyor belt accounts for the largest proportion of the multiple running resistance of the conveyor and is more than 50%. Therefore, it is necessary to study the indentation resistance caused by the contact between the rollers and the conveyor belt in order to save energy and optimize the design of the belt conveyor [14].

The top and bottom coverings of conveyor belts are generally made of natural viscoelastic materials, synthetic viscoelastic materials, and mixtures of various viscoelastic materials. Rubber, as a typical viscoelastic material, is widely used for the upper and lower coverings of conveyor belts [15]. The upper cover layer serves to convey and carry the material, while the lower cover layer transfers the load to the rollers. During the operation of the belt conveyor, the contact parts of the lower cover and rigid rollers are deformed under the load and the self-weight of the belt. Because of the viscoelasticity of the conveyor belt made of rubber, the contacting part shows delayed stress, which results in uneven distribution of stress around the contacting part and causes indentation resistance in the contacting part of the roller and the lower cover of the conveyor belt [16].

In summary, it is important to investigate the indentation resistance of the contact between the rollers and the conveyor belt to optimize the energy-saving design of the belt conveyor. However, the generation of indentation resistance is closely related to the viscoelastic properties of the conveyor belt, so the analysis of indentation resistance must be preceded by an in-depth study of the viscoelastic mechanical properties of rubber materials [17]. At present, some scholars have used numerical calculations based on the three-element Maxwell model for viscoelastic materials to analyze the indentation resistance under common operating conditions [18], but the parameters in the three-element Maxwell model are not suitable for different viscoelastic materials. In this study, a new research method will be used to test the relaxation modulus of different viscoelastic materials based on the three-element Maxwell model to achieve a parametric characterization of the relaxation modulus of different viscoelastic materials [19, 20].

2. Related Work

As a typical viscoelastic material, the relaxation modulus of permafrost is closely related to the analysis of mechanical properties of viscoelastic materials. In [21], the relaxation modulus was calculated under the nonlinear Kelvin model based on the theory of half-space viscoelasticity and fractional-order differential integration theory. The accuracy of the prediction of relaxation modulus of permafrost based on the spherical indentation test was evaluated by processing the results of the creep test under specific loading conditions. In [22], a new relaxation modulus solution method under the generalized Maxwell model was proposed using the optimal LM algorithm, which is to fit the relaxation modulus parameters corresponding to the experimental data or the KWW formula, and this method can be used to effectively avoid negative values of the relaxation modulus parameters of viscoelastic materials.

3. Theory and Methods for Testing the Relaxation Modulus of Viscoelastic Materials

The relaxation modulus of viscoelastic materials is an important index to describe the relaxation properties of materials. In this section, a method for testing the relaxation modulus and a method for solving the relaxation modulus parameters are proposed. The Hertzian contact theory [23] and the Boltzian superposition principle [24] are investigated to derive the theoretical equation between the stress and the relaxation modulus of a viscoelastic material subjected to a certain strain. A relaxation modulus test method is proposed based on the derived theoretical equations, and a relaxation modulus parameter solution method is proposed based on this test method.

$$\begin{aligned} r^2 + (R_1 - z_1)^2 &= R_1^2, \\ r^2 + (R_2 - z_2)^2 &= R_2^2. \end{aligned} \tag{1}$$

If z_1, z_2 is very small, then

$$\begin{aligned} z_1 &= \frac{r^2}{2R_1}, \\ z_2 &= \frac{r^2}{2R_2}. \end{aligned} \tag{2}$$

That is, the distance between points M and N is

$$\begin{aligned} z_1 + z_2 &= \frac{r^2}{2R_1} + \frac{r^2}{2R_2} \\ &= \frac{(R_1 + R_2)r^2}{2R_1R_2}. \end{aligned} \tag{3}$$

If we take $R_1 \longrightarrow \infty$, then $z_1 = 0$; we can represent the case where the plane is in contact with the sphere, and the distance between the points M and N is $r^2/2R_2$.

If two balls are squeezed by a pressure of magnitude P in the direction of the line connecting the centers of the two balls,

a local deformation occurs near the point O, forming a small circular contact area; because the deformation is small, the radius a and the proximity h of the contact area are much smaller than R_1 and R_2. According to the theoretical derivation, the radius a and the proximity h of the contact region are

$$a = \left[\frac{3}{4}\frac{R_1R_2}{R_1+R_2}\left(\frac{1-\mu_1^2}{E_1}+\frac{1-\mu_2^2}{E_2}\right)P\right]^{1/3}, \tag{4}$$

$$h = \left[\frac{9}{16}\frac{R_1+R_2}{R_1R_2}\left(\frac{1-\mu_1^2}{E_1}+\frac{1-\mu_2^2}{E_2}\right)^2P^2\right]^{1/2}, \tag{5}$$

where μ_1 and μ_2 are Poisson's ratios of the two rigid spheres, respectively; E_1 and E_2 are the moduli of elasticity of the two rigid spheres, respectively. If we make $k_1 = 1-\mu_1^2/\pi E_1$, $k_2 = 1-\mu_2^2/\pi E_2$, (4) and (5) can be simplified as

$$\begin{aligned} a &= \left[\frac{3\pi R_1R_2P(k_1+k_2)}{4(R_1+R_2)}\right]^{1/3}, \\ h &= \left[\frac{9\pi^2P^2(R_1+R_2)(k_1+k_2)^2}{16R_1R_2}\right]^{1/3}. \end{aligned} \tag{6}$$

The maximum force between the two spheres in the contact area is q_0.

$$q_0 = \frac{3P}{2\pi a^2}, \tag{7}$$

where P is the pressure acting on the two spheres; a is the radius of the circular contact area. We can extend the Hertzian contact theory to the test of viscoelastic materials with a rigid spherical indenter in contact with a flat viscoelastic material. In contrast to viscoelastic materials, the spherical indenter has an extremely large modulus of elasticity and can be considered as $E_1 \longrightarrow \infty$; meanwhile, for planar viscoelastic materials, it can be considered as a sphere with infinite radius, i.e., $R_2 \longrightarrow \infty$.

As a result, in the case of a rigid spherical indenter in contact with a flat viscoelastic material, we can obtain the following equations:

$$\begin{aligned} E_2 &= \frac{3R_1P\left(1-\mu_2^2\right)}{4a^3}, \\ h &= \frac{3P\left(1-\mu_2^2\right)}{4E_2a} \\ &= \sqrt[3]{\frac{9P^2\left(1-\mu_2^2\right)^2}{16E_2^2R_1}}, \end{aligned} \tag{8}$$

$$P = \frac{4}{3}\frac{E_2}{1-\mu_2^2}\sqrt{R_1}h^{3/2}, \tag{9}$$

where E_2 and μ_2 represent the elastic modulus and Poisson's ratio of the viscoelastic material, respectively; R_1 is the radius of the spherical indenter; P is the pressure of the spherical indenter on the viscoelastic material; a is the radius of the circular contact area; h is the indentation amount of the spherical indenter on the viscoelastic material. According to (9), we can find the relationship between the indentation amount and pressure when the spherical indenter is pressed into a flat viscoelastic material.

In order to study the relationship between strain, stress, and time in viscoelastic materials, Hunter obtained the relationship between the pressure and depth of indentation and creep flexibility in the case of contact between a spherical indenter and a viscoelastic material based on the Hertzian contact theory and Boltzmann superposition principle combined with genetic integration operators [24]:

$$h^{3/2}(t) = \frac{3(1-\nu)}{8\sqrt{R}}\int_0^t J(t-\theta)\frac{\mathrm{d}P(\theta)}{\mathrm{d}\theta}\mathrm{d}\theta, \tag{10}$$

where $h(t)$is the indentation depth; ν is Poisson's ratio of the material; R is the radius of the spherical indenter; $J(t)$ is the creep flexibility of the material; $P(t)$ is the pressure profile.

Later, Lee and Radok proposed the relationship between pressure and indentation volume and creep flexibility in the experiments of conical indenter into viscoelastic materials:

$$h(t) = \frac{\pi(1-\nu)\tan\alpha}{4}\int_0^t J(t-\theta)\frac{\mathrm{d}P(\theta)}{\mathrm{d}\theta}\mathrm{d}\theta, \tag{11}$$

where α is the angle between the tapered indenter and the substrate plane; $h(t)$ is the press-in depth; ν is Poisson's ratio of the material; $J(t)$ is the creep flexibility of the material; $P(t)$ is the pressure curve.

(11) and (12) give the relationship between the pressure on the material and the depth of compression and the creep flexibility from the perspective of the conical and spherical indenter into the viscoelastic material, respectively, and provide a theoretical basis for the study of creep flexibility of viscoelastic materials. In order to simplify the integration operation, domestic and foreign scholars use the ramp stress loading method, i.e., $\mathrm{d}P(\theta)/\mathrm{d}\theta = \nu_0$ (constant) is made to simplify the above two equations:

$$h^{3/2}(t) = \frac{3(1-\nu)\nu_0}{8\sqrt{R}}\int_0^t J(t-\theta)\mathrm{d}\theta, \tag{12}$$

$$h(t) = \frac{\pi(1-\nu)\tan\alpha\nu_0}{4}\int_0^t J(t-\theta)\mathrm{d}\theta. \tag{13}$$

According to (13) and (14), a conical indenter or a spherical indenter is pressed into a viscoelastic planar material by ramp stress loading, and the data of the depth of indentation are obtained; then, the creep flexibility of the material is obtained by processing the data, and the parametric solution of the creep flexibility is completed. In 1985, Jonson K, a British scholar, proposed the relationship between the stress of the material and the indentation depth and relaxation modulus of the indenter in the case of a spherical and conical indenter pressed into a half-space viscoelastic material based on the Hertzian contact theory and Boltzmann superposition principle [25]. The following

(14) and (15) represent the relationship between the quantity in the case of conical and spherical indenter, respectively:

$$P(t) = \frac{2\tan\theta}{\pi\left(1-\mu^2\right)} \int_0^t E(t-\tau)\frac{\mathrm{d}\alpha^2(\tau)}{\mathrm{d}\tau}\mathrm{d}\tau, \tag{14}$$

$$P(t) = \frac{4\sqrt{R}}{3\left(1-\mu^2\right)} \int_0^t E(t-\tau)\frac{\mathrm{d}\alpha^{3/2}(\tau)}{\mathrm{d}\tau}\mathrm{d}\tau, \tag{15}$$

where θ represents the angle between the tapered indenter and the substrate plane; $\alpha(t)$ represents the indentation depth; μ is Poisson's ratio of the material; R represents the radius of the rigid spherical indenter; $E(t)$ represents the relaxation modulus of the material; $P(t)$ is the stress of the material.

According to (15), we can obtain the relaxation modulus of a viscoelastic material based on the relationship between pressure and depth of indentation when the indenter is pressed into the material. However, since the integral calculation is too complicated, this study proposes a new theory and method for testing the relaxation modulus of viscoelastic materials with a simple calculation by referring to the above-mentioned method for testing the creep flexibility of viscoelastic materials with a spherical indenter.

For (15), to simplify the integral calculation, let $\mathrm{d}\alpha^{3/2}(\tau)/\mathrm{d}\tau = v_0$ (a constant), then

$$\alpha(t) = \left(v_0 t\right)^{2/3}, \tag{16}$$

$$P(t) = \frac{4\sqrt{R}v_0}{3\left(1-\mu^2\right)} \int_0^t E(t-\tau)\mathrm{d}\tau, \tag{17}$$

where μ is Poisson's ratio of the material; v_0 is the constant; R represents the radius of the rigid spherical indenter; $E(t)$ represents the relaxation modulus of the material; $P(t)$ is the stress of the material.

Equation (16) describes the relationship between the stress and the relaxation modulus of a viscoelastic material when a spherical indenter is pressed into the material with the motion law specified in (17), which greatly simplifies the calculation of the relaxation modulus of the material. In this paper, we will use (17) as the theoretical basis for the study of relaxation modulus of materials, conduct relaxation modulus test experiments by pressing a spherical indenter into a viscoelastic material according to a specific motion law, and then solve the relaxation modulus of viscoelastic materials based on the experimental data.

4. Experimental and Data Analysis of Relaxation Modulus Testing of Viscoelastic Materials

The relaxation modulus of viscoelastic materials was tested, and the expression of the relaxation modulus function based on the three-element Maxwell model was obtained by using the data fitting method to realize the parametric characterization of the relaxation modulus. The calibration of the sensor, the design of the experimental procedure, and the processing of the experimental data were carried out. The experimental curves were fitted using the origin curve fitting function. An error analysis was performed to verify the reliability of the device and the accuracy of the fitting results.

4.1. Acquisition and Processing of Experimental Data. When the distance between the inductor plate and the eddy current displacement sensor probe is between 1.5 mm and 3.5 mm, the output voltage of the eddy current sensor has a good linear relationship with the input displacement, so the linear interval of this eddy current displacement sensor is between 1.5 mm and 3.5 mm from the probe, and the change value of the output voltage of the eddy current displacement sensor is 0.5 mm per interval in this interval. The average value of the voltage change is 0.394 V, so the sensitivity of the eddy current displacement sensor is 0.788 V/mm, which can also be expressed as 1.269 mm/V. Similarly, the S-type pull pressure transducer is calibrated. The sensitivity of the S-type pull pressure transducer is 1.46 mV/g, which can also be expressed as 689.688 g/V.

In summary, by calibrating the S-type pull pressure transducer and eddy current transducer, we can get the sensitivity and linearity interval of the two transducers, and the zero point of the transducer can be determined according to the actual experimental situation, and the actual pressure and displacement data can be read by imputing the sensitivity and zero point of the two transducers into the Labview data reading program.

4.2. Experimental Procedure. After completing the calibration of the S-type tensile transducer and eddy current displacement transducer, we can conduct the viscoelastic material relaxation modulus experiment.

4.3. Analysis and Processing of Experimental Data. Later, the viscoelastic material relaxation modulus test bench is set up. The experimental data are collected and saved in the computer through the Labview data acquisition program. In the process of data acquisition, we can see from the front panel of the acquisition program in real time that as the stepper motor rotates, the rigid ball head gradually presses into the viscoelastic rubber material, and the voltage value displayed in channel 0 to express the amount of ball head pressed into the rubber material becomes larger, and the voltage value displayed in channel 1 to express the change of stress response also becomes larger.

After collecting the experimental data, stored experimental data are read using the data reading program written to obtain the motion curve and stress response curve of the rigid ball head pressed into the rubber material for this experiment. According to the above study, the sensitivity and zero point values of the eddy current sensor and S-type displacement sensor should be set in the reading program before reading the data, i.e., the voltage data of both channels should be subtracted from the corresponding zero point and then multiplied by the sensitivity of the two sensors.

Since the contact between the indenter and the measured material has been adjusted before the experiment, the

voltage values of the two channels collected at the beginning of the experiment are the zero point values of the sensors, where the zero point value and sensitivity of the eddy current sensor are −1.8945 V and −1.269 mm/V, respectively, and the zero point value and sensitivity of the S-type pull-pressure sensor are 0.724 V and 689.655 g/V, respectively. Since the data are collected on the number of data points as the horizontal coordinate, it is necessary to divide the horizontal coordinate by the set sampling frequency when processing the data to obtain the data curve with the horizontal coordinate in time. According to the experimental data, the variation curves of indentation depth and stress response of rubber material with time can be obtained, as shown in Figure 1. The curve of the depth of spherical indenter into the viscoelastic rubber material as a function of time is shown in Figure 1.

In Figure 1, the curve depicted in series 1 is the theoretical compression depth curve to be followed when the spherical indenter is pressed into the viscoelastic rubber material, and the curve depicted in series 2 is the compression depth curve when the spherical indenter is pressed into the viscoelastic rubber material measured by the experiment. The error between the real data points and the theoretical data points is very small, thus verifying the reliability of the experimental setup and the accuracy of the control system.

The stress response curve of the spherical indenter with time when pressing into the 70HA rubber material is shown in Figure 2.

According to the formula of the Maxwell model, the stress response curve $P(t)$ experimentally obtained from the ball head pressed into the viscoelastic rubber material can be processed, i.e.,

$$f(t) = \frac{3P(t)\left(1-\mu^2\right)}{4\sqrt{R}v_0}, \tag{18}$$

where $P(t)$ is the stress response curve; $\mu = 0.5$ is Poisson's ratio of the rubber material; $R = 0.004$ m is the radius of the spherical indenter used in this experiment; v_0 is determined by the law of motion of the indenter, and its value is $10^{-(15/2)}$ after unit unification.

Meanwhile, the relationship between the material relaxation modulus parameter and $f(t)$ can be obtained as

$$f(t) = E_0 t + \sum_{i=1}^{N}\left[\tau_i E_i\left(1 - e^{-(t/\tau_i)}\right)\right], \tag{19}$$

where $E(t)$ is the relaxation modulus function of materials; E_0 and E_i are the parameters of relaxation modulus; τ_i is the delay time; N is the number of components.

The relationship between $f(t)$ and each relaxation modulus parameter under the three-element Maxwell model is as follows:

$$f(t) = E_0 t + \tau_1 E_1\left(1 - e^{-(t/\tau_1)}\right). \tag{20}$$

According to (20) and the 70 HA rubber stress response curve $P(t)$, the curve of $f(t)$ as a function of time is shown in Figure 3.

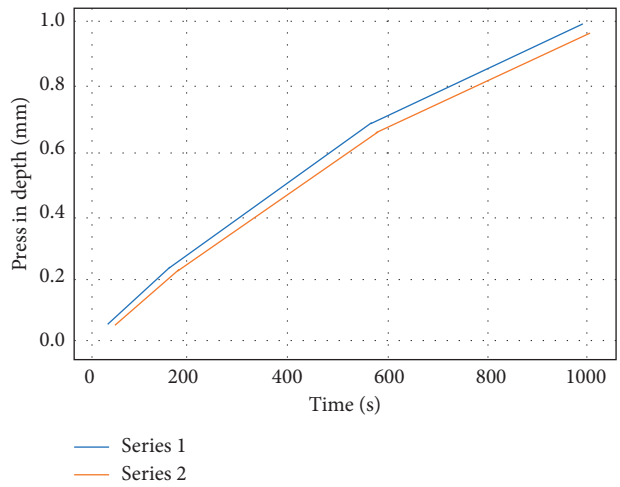

Figure 1: Depth of ball indentation curve with time.

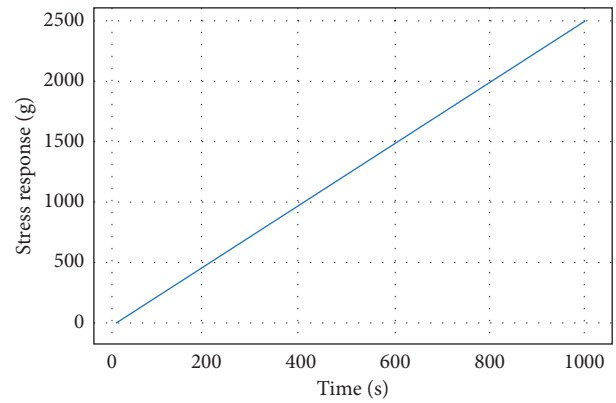

Figure 2: Stress response curve of 70 HA rubber with time.

The $f(t)$ curves of rubber materials with Shore hardnesses of 65 HA and 75 HA can be obtained by processing the measured experimental data according to the above experimental procedures, as shown in Figure 4.

In Figure 4, series 1 shows the $f(t)$ curve for a rubber material with a Shore hardness of 65 HA; series 2 shows the $f(t)$ curve for a rubber material with a Shore hardness of 75 HA as a function of time.

4.4. Error Analysis of Fitting Results. In order to study the accuracy of the fitting results, we substitute the parameters of the relaxation modulus function obtained by fitting the data into the equation, calculate the data points at different times, and then compare them with the experimental data points and make the difference to obtain the absolute error and relative error of the fitting results. The absolute and relative errors of the fitting results of the relaxation modulus parameters for the rubber material with Shore hardness of 70 HA are shown in Figures 5 and 6, respectively.

From the above absolute and relative error plots of the relaxation modulus parameter fitting results, we can see that it is feasible to use the data fitting method to solve the

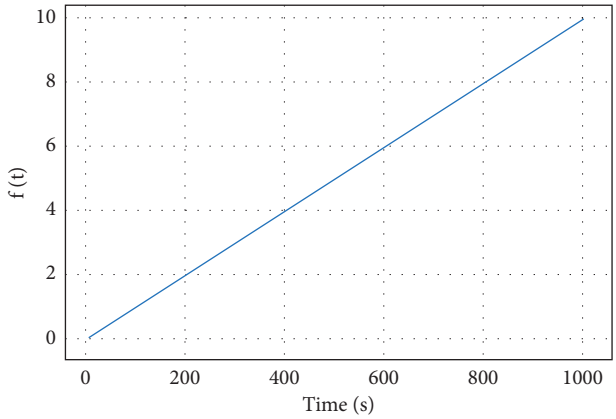

Figure 3: 70 HA rubber $f(t)$ curve.

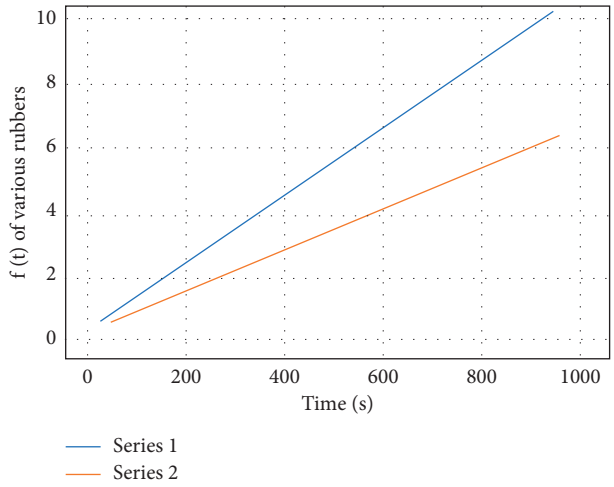

Figure 4: Curves of different rubber materials.

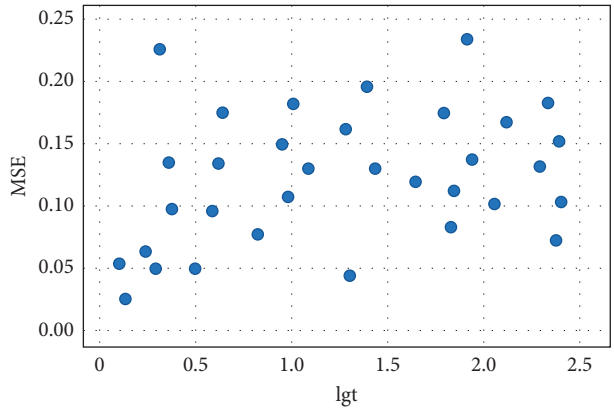

Figure 5: Absolute error in the fitting results of the relaxation modulus parameters of rubber type 70 HA.

relaxation modulus parameter, and the error caused by this parameter solving method is very small and satisfies the requirements.

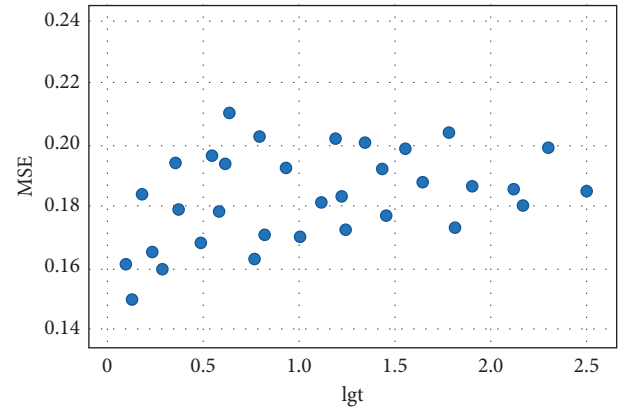

Figure 6: Relative error in the fitting results of the relaxation modulus parameters of rubber type 70 HA.

5. Conclusions

In this paper, relaxation modulus tests were conducted on three viscoelastic materials, and relaxation modulus expressions were obtained for the three-element Maxwell model. Calibration of eddy current sensor and force sensor was studied. And a reasonable experimental procedure was designed to test the relaxation modulus of various viscoelastic rubber materials. The experimental data were fitted and analyzed to obtain a good fitting curve. And the relaxation modulus parameters of various materials were solved under the three-element Maxwell model. The experimental setup and parameter fitting results were analyzed to verify the feasibility and accuracy of the results [26].

Data Availability

The data underlying the results presented in this study are included within the manuscript.

Conflicts of Interest

The authors declare that they have no conflicts of interest.

References

[1] V. Crecea, A. L. Oldenburg, X. Liang, T. S. Ralston, and S. A. Boppart, "Magnetomotive nanoparticle transducers for optical rheology of viscoelastic materials," *Optics Express*, vol. 17, no. 25, Article ID 231, 2009.

[2] Q. Xu and B. Engquist, "A mathematical model for fitting and predicting relaxation modulus and simulating viscoelastic responses," *Proceedings of the Royal Society A: Mathematical, Physical & Engineering Sciences*, vol. 474, no. 2213, Article ID 20170540, 2018.

[3] M. D. Paola, V. Fiore, F. P. Pinnola, and V. Antonino, "On the influence of the initial ramp for a correct definition of the parameters of fractional viscoelastic materials," *Mechanics of Materials*, vol. 69, no. Feb, pp. 63–70, 2014.

[4] Y. He, "Fitting methods based on custom neural network for relaxation modulus of viscoelastic materials," *International Journal of Performability Engineering*, vol. 15, no. 1, 2019.

[5] Z. M. Xie, J. Zhang, and Y. S. Wang, "A comparative study on the viscoelastic models for rubbery materials," *Advanced Materials Research*, vol. 905, pp. 176–180, 2014.

[6] S. Mun, "Determining the dynamic modulus of a viscoelastic asphalt mixture using an impact resonance test with damping effect," *Research in Nondestructive Evaluation*, vol. 26, no. 4, pp. 189–207, 2015.

[7] K. Ishihara, "Effect OF rate OF loading ON the modulus OF deformation OF materials exhibiting viscoelastic behaviors [j]," *Transactions of the Japan Society of Civil Engineers*, vol. 1965, no. 117, pp. 35–50, 2009.

[8] A. H. Jiménez, B. V. Jara, and J. H. Santiago, "Relaxation modulus in the fitting of polycarbonate and poly(vinyl chloride) viscoelastic polymers by a fractional Maxwell model," *Colloid & Polymer Science*, vol. 280, no. 5, pp. 485–489, 2002.

[9] F. Cortés and M. J. Elejabarrieta, "Modelling viscoelastic materials whose storage modulus is constant with frequency [J]," *International Journal of Solids and Structures*, vol. 43, no. 25-26, pp. 7721–7726, 2006.

[10] W. Li, W. Meng, and S. Furnell, "Exploring touch-based behavioral authentication on smartphone email applications in IoT-enabled smart cities[J]," *Pattern Recognition Letters*, vol. 144, no. 5, 2021.

[11] M. S. Commisso, J. Martínez-Reina, and J. Mayo, "Numerical simulation of a relaxation test designed to fit a quasi-linear viscoelastic model for temporomandibular joint discs," *Proceedings of the Institution of Mechanical Engineers - Part H: Journal of Engineering in Medicine*, vol. 227, no. 2, pp. 190–199, 2013.

[12] Y. Zhang and M. N. Toksoz, "Impact of the cracks lost in the imaging process on computing linear elastic properties from 3D microtomographic images of Berea sandstone," *Geophysics*, vol. 77, no. 2, p. 95, 2011.

[13] K. Zhang, T. Qu, D. Zhou et al., "IoT-enabled dynamic lean control mechanism for typical production systems," *Journal of Ambient Intelligence and Humanized Computing*, vol. 10, no. 3, pp. 1009–1023, 2019.

[14] Y. Feng, P. Bayly, J. Huang, and G. R. Cliff, "TH-C-141-05: a simulation study to investigate the potential of using magnetic resonance elastography (mre) to differentiate recurrent tumor and radiation necrosis," *Medical Physics*, vol. 40, no. 6, p. 540, 2013.

[15] A. I. Awad, S. Furnell, A. M. Hassan, and T. Theo, "Special issue on security of IoT-enabled infrastructures in smart cities," *Ad Hoc Networks*, vol. 92, Article ID 101850.2, 2019.

[16] Q. Zhang, Z. Luo, C. Zhao, B. A. Jang, and R. Zhang, "Modeling the Cyclic Relaxation Behavior of the Artificial discontinuity," *Mechanics of Advanced Materials and Structures*, vol. 28, pp. 1–7, 2019.

[17] O. H. Campanella, "Note: on the relationship between the dynamic viscosity and the relaxation modulus of viscoelastic liquids," *Journal of Rheology*, vol. 31, no. 6, pp. 511–513, 2000.

[18] H. T. Banks, N. G. Medhin, and G. A. Pinter, "Modeling of viscoelastic shear: a nonlinear stick-slip formulation," *Dynamic Systems and Applications*, vol. 17, no. 2, p. 23, 2006.

[19] X. Qinwu and E. Bjorn, "A mathematical model for fitting and predicting relaxation modulus and simulating viscoelastic responses," *Proceedings of the Royal Society. Mathematical, physical and engineering sciences*, vol. 474, no. 2213, 2018.

[20] K. Gabry and A. Szymański, "The evaluation of the initial shear modulus of selected cohesive soils," *Studia Geotechnica et Mechanica*, vol. 37, no. 2, 2015.

[21] B. Huang, R. J. Bathurst, K. Hatami, and T. M. Allen, "Influence of toe restraint on reinforced soil segmental walls," *Canadian Geotechnical Journal*, vol. 47, no. 8, pp. 885–904, 2010.

[22] E. D. Manga, H. Blasco, P. Da-Costa et al., "Effect of gas adsorption on acoustic wave propagation in MFI zeolite membrane materials: experiment and molecular simulation," *Langmuir*, vol. 30, no. 34, Article ID 10343, 2014.

[23] W. Zhang, B. Cui, X. Gu, and Q. Dong, "Comparison of relaxation modulus converted from frequency- and time-dependent viscoelastic functions through numerical methods," *Applied Sciences*, vol. 8, no. 12, 2018.

[24] E. F. Oleinik, I. A. Chmutin, and N. G. Ryvkina, "Effect of plastic deformation on the character of micro-brownian motions in glassy poly(methyl methacrylate)," *Polymer Science - Series A*, vol. 54, no. 6, pp. 465–475, 2012.

[25] R. Hellbach, K. Klein, and K. Hribernik, "IoT-enabled communication systems in testing environments," *Procedia Manufacturing*, vol. 52, pp. 85–88, 2020.

[26] R. L. Hou, J. X. Peng, J. H. Zhang, and P. Zhou, "Modification of SCG model for shear modulus calculation," *Journal of Wuhan University of Technology*, vol. 31, no. 16, pp. 87–90, 2009.